Proc. Natl. Acad. Sci. USA
Vol. 93, pp. 6264–6268, June 1996
Biophysics

Probing the interaction between two single molecules: Fluorescence resonance energy transfer between a single donor and a single acceptor

T. HA*†‡, TH. ENDERLE*‡, D. F. OGLETREE‡, D. S. CHEMLA*†‡, P. R. SELVIN§¶‖, AND S. WEISS*‡‖

*Molecular Design Institute, ‡Materials Sciences Division, and §Life Sciences Division, Lawrence Berkeley National Laboratory, 1 Cyclotron Road, Berkeley, CA 94720; and †Physics Department and ¶Department of Chemistry, University of California, Berkeley, CA 94720

Communicated by I. Tinoco, Jr., University of California, Berkeley, CA, March 5, 1996 (received for review January 17, 1996)

ABSTRACT **We extend the sensitivity of fluorescence resonance energy transfer (FRET) to the single molecule level by measuring energy transfer between a single donor fluorophore and a single acceptor fluorophore. Near-field scanning optical microscopy (NSOM) is used to obtain simultaneous dual color images and emission spectra from donor and acceptor fluorophores linked by a short DNA molecule. Photodestruction dynamics of the donor or acceptor are used to determine the presence and efficiency of energy transfer. The classical equations used to measure energy transfer on ensembles of fluorophores are modified for single-molecule measurements. In contrast to ensemble measurements, dynamic events on a molecular scale are observable in single pair FRET measurements because they are not canceled out by random averaging. Monitoring conformational changes, such as rotations and distance changes on a nanometer scale, within single biological macromolecules, may be possible with single pair FRET.**

Fluorescence resonance energy transfer (FRET) has found wide use in structural biology, biochemistry, and polymer science for measuring distances in the 10- to 80-Å range (1–5). In FRET, energy is transferred from a donor molecule to an acceptor molecule via an induced-dipole, induced-dipole interaction, with the transfer efficiency E depending on the inverse-sixth-power of the distance R between the donor and acceptor: $E = 1/(1+[R/R_o]^6)$, where R_o is the distance at which 50% of the energy is transferred. R_o is a function of the properties of the dyes and the relative orientation of their dipole moments: $R_o = [8.79 \times 10^{-5} J(\lambda)\, \phi_D\, n^{-4}\, \kappa^2]^{1/6}$ [Å]. $J(\lambda)$ is the spectral overlap of donor emission and acceptor absorption [$nm^4 \cdot M^{-1} \cdot cm^{-1}$], ϕ_D is the donor quantum yield, n is the index of refraction of the medium, and κ^2 is a geometrical factor which accounts for the relative orientation of the two dipoles.

Near-field scanning optical microscopy (NSOM) (6–8) is a relatively new technique that allows optical measurements with sub-wavelength resolution. It is based on a probe consisting of a very small (sub-wavelength) aperture that is placed in close proximity (in the near field; <10 nm) to the sample under study. By using the probe as an excitation source, fluorescence of a single molecule has been detected (9). The emission spectra (10) and excited state lifetime (11–13) of a single molecule have also been measured. Another important aspect of near-field detection is that the optical radiation in the near field has an electric field component along its direction of propagation (in contrast to far-field radiation). This allows mapping the transition dipole moment orientation of a single fluorescent molecule in three dimensions (9).

The marriage between FRET and NSOM offers many potential advantages when distance and orientation information is required on a molecular level. Here we list several. (*i*) Because the orientation of donor and acceptor can potentially be measured, the uncertainty in κ^2, which is often a large source of uncertainty in distance determination in conventional FRET measurements, is minimized. (*ii*) In addition to measuring κ^2, the knowledge of donor and acceptor orientations can be of importance for measuring rotational dynamics. (*iii*) Conventional (i.e., ensemble) FRET measurements, which rely on signal averaging over many molecules, cannot detect dynamic events such as relative motion between donor and acceptor molecules when these event are not synchronized between molecules, as is often the case. The ability to measure FRET on a single pair potentially allows the study of time-dependent phenomena such as protein and molecular motor conformational changes. (*iv*) With ensemble-FRET, great care must be taken to purify the complex labeled with both donor and acceptor. The presence of small amounts of single-species complexes (donor-only or acceptor-only) can greatly affect the results and interpretation of the measurements. With single pair FRET (spFRET), this problem is eliminated since one complex is measured at a time, and the donor-acceptor labeled complex can be easily distinguished from single species by their characteristic spectral properties.

MATERIALS AND METHODS

DNA Synthesis. As a model system, we measured energy transfer between a single tetramethylrhodamine dye molecule (the donor) and a single Texas Red dye molecule (the acceptor) attached to the 5′ ends of hybridized, complementary DNA of length 10 or 20 bases. DNA oligomers of the appropriate length were synthesized by standard phosphoramidite technology with a 6-carbon aminophosphoramidite (Glen Research, Sterling, VA) placed at the 5′ end. The donor strand, labeled with the 5-isomer of tetramethylrhodamine isothiocyanate (TMR; Molecular Probes), was 5′-CCACTCTAGG-3′ and 5′-CCACTGCACTCGCTGCTAGG-3′ for the 10- and 20-mer, respectively. Complementary oligonucleotides were synthesized and labeled with Texas Red (TR; Molecular Probes). Unlabeled strands were also synthesized. All DNA were reverse-phase HPLC purified. For the spectroscopy, strands were dissolved in buffer containing 10 mM Tris·HCl (pH 8.0), 15 mM $MgCl_2$, and 100 mM NaCl and hybridized by mixing, heating to 65°C, and cooling to 5°C over 15 min at ≈0.2 μM. Donor-only and acceptor-only samples were also made by hybridizing the TMR-DNA or TR-DNA to an unlabeled complement. (We denote the doubly labeled samples as TMR-10-TR and TMR-20-TR; the singly labeled double-stranded

The publication costs of this article were defrayed in part by page charge payment. This article must therefore be hereby marked "*advertisement*" in accordance with 18 U.S.C. §1734 solely to indicate this fact.

Abbreviations: FRET, fluorescence resonance energy transfer; sp-FRET, single pair FRET; NSOM, near-field scanning optical microscopy; TMR, tetramethylrhodamine isothiocyanate; TR, Texas Red; APS, amino-propyl-salanized; APD, avalanche photodiode; FWHM, full-width half-maximal; CCD, charge-coupled device.

‖To whom reprint requests should be addressed.

samples are denoted as TMR-10, TR-10 and TMR-20, TR-20, respectively). A titration measuring donor-quenching of TMR-labeled DNA upon addition of TR-labeled DNA was used to verify concentrations and the extent of hybridization. For the TMR-DNA-TR sample, an ≈1:1 ratio of DNA strands was used; for the TMR-only and TR-only sample, a 2-fold excess of unlabeled, complementary strand was used to increase the probability that all dye-labeled DNA was in double-stranded form.

Solution (Ensemble) FRET Measurements. Conventional solution (ensemble) measurements were made on a Spex Industries (Mutuchen, NJ) fluorolog steady-state fluorimeter. Energy transfer was determined by comparing the relative fluorescence spectra and intensities of TMR-DNA-TR, TMR-DNA, and TR-DNA and measuring donor-quenching and sensitized emission according to standard methods (see refs. 1–5). We measured 65% energy transfer on the TMR-10-TR sample, which indicated that the donor and acceptor were ≈40 Å apart in solution, and 32% energy transfer for the 20 mer sample, which indicated 59-Å separation in solution. Estimated distances were based on an R_o of 52 Å ($R = R_o[E^{-1} - 1]^{1/6}$). R_o was calculated by using a measured spectral overlap of $J = 4.2 \times 10^{15}$ nm^4·M^{-1}·cm^{-1}, a TMR quantum yield of 0.25, a κ^2 of 2/3, and an index of refraction of 1.33. The polarization anisotropy of the TMR-20 and TR-20 were also measured and found to be 0.17 and 0.16, respectively, which indicated that the assumption of $\kappa^2 = 2/3$, and therefore the derived-distances, are only rough approximations. In addition, the relatively high anisotropy measurements and the large amount of energy transfer on the 20-mer indicate that, in solution, the dyes are strongly interacting with the DNA, and the flexible 6-carbon linkers may enable the dyes to fold back so they are closer together than their points of attachment to the DNA.

NSOM–FRET Measurements. For NSOM–FRET measurements, the DNA was dried on amino-propyl-silanized (APS) glass. Slides were made by washing glass coverslips for 2 min in a 1.5% solution (in H_2O) of 3-aminopropyl-triethoxysilane (United Chemical Technologies, Bristol, PA), followed by washing with H_2O, and then drying in a desiccator. Before use, the APS solution was filtered through a 0.2-μm filter and stored in hydrofluoric acid-cleaned glassware. A 0.3-μl drop of 10–50 nM double-stranded DNA solution in buffer was spread on APS-treated coverslips in a 4°C cold room, followed by washing with H_2O and drying with nitrogen gas. This preparation resulted in roughly 10 molecules per square micrometer.

The NSOM was built into a Zeiss Axioskop optical microscope. The optical path was similar to the ones described in refs. 9 and 10. The 514-nm line of an Ar^+ ion laser, sent through a tapered aluminumn-coated optical fiber, was used for excitation. Emission from the sample plane was imaged onto the various detectors with additional optics. Shear force feedback was used to maintain tip-sample separation at 5 nm (±1 nm). (A 1.3-μm semiconductor laser is used to monitor the dithering amplitude of the tip.) Avalanche photodiode (APD) detectors were used for fluorescence imaging, and a liquid nitrogen cooled, back-thinned charge-coupled device (CCD) camera, attached to a spectrometer, was used for emission spectroscopy. For one-color imaging, only one APD detector was used. For two-color imaging, a dichroic mirror was used to spectrally separate the emission from donor and acceptor. In this case two APDs were used for the two channels.

We note that two-color imaging and single molecule (pair) spectroscopy are complementary techniques with different time/spectral resolutions (usually 50 nm/10 ms for the first, 1 nm/5 s for the latter).

RESULTS AND DISCUSSION

As a reference, emission spectra were taken on singly labeled DNA molecules (TMR-10, TR-10). Fig. 1 is a scatter plot of these emission spectra. Typical spectrum for each fluorophore, fitted to a sum of two Gaussians, are shown as *Insets*. Each single molecule is represented by the peak wavelength and FWHM of its emission spectrum. The average peak position and FWHM for the donor-only and acceptor-only are 566.4 ± 9.1 nm, FWHM 34.8 ± 4.9 nm and 601.6 ± 12.2 nm, FWHM 34.1 ± 4.9 nm, respectively. The variance in these numbers reflects the inhomogeneity due to different local environment. The 35-nm difference in average peak position between donor-only and acceptor-only is three times the uncertainty in their peak positions, indicating that donor-only and acceptor-only spectra can be easily distinguished.

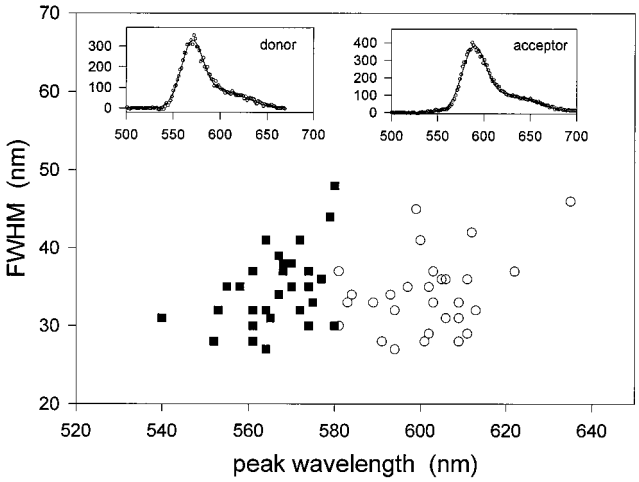

FIG. 1. Scatter plot of emission spectra of donor-labeled DNA and acceptor-labeled DNA. Filled squares are donors and empty circles are acceptors. Each single molecule is represented by the peak wavelength and full-width half-maximum (FWHM) of its emission spectrum. Typical spectrum for donor and acceptor, fit to a sum of two Gaussians, are shown as *Insets*. Single molecule (or pair of molecules) spectrum was taken in the following way: a fluorescence image (one color or two color) was taken. The probe was positioned over a molecule in the field of view by adjusting the offset voltages on the scanner. The reading of the APDs was optimized. The light was then redirected to a spectrometer. CCD detector binning was used (five pixels = 1 bin), resulting in 1.5-nm spectral resolution. Laser excitation was chopped with a shutter that is synchronized with the CCD shutter to minimize unnecessary exposure of molecules. NSOM probe tips with aperture sizes ranging between 100 and 200 nm were used, delivering 5 to 40 nW of excitation. No heating effects were observed on single molecule spectra within this excitation range. Integration time for each spectral scan was 5 s.

Near-field fluorescence images and emission spectra were taken on the double-stranded DNA molecules (labeled with donor-only, with acceptor-only, or with both donor and acceptor). Confirmation that emission was arising from only a single fluorophore or single pair of fluorophores was made in two ways: (*i*) single fluorophores had a well-defined orientation characteristic of a single electric dipole moment (checked at two orthogonal linearly polarized excitations) (9), and (*ii*) photodestruction of fluorescence emission was sudden and led to background (near-zero) fluorescence (9).

Fig. 2 presents images obtained with linearly polarized light on the TMR-10-TR sample. The digitized red-green-blue values of donor image (Fig. 2*a*, green) and acceptor image (Fig. 2*b*, red) are combined to form a composite image (Fig. 2*c*). Green or red color spots in Fig. 2*c* represents emission primarily from donor or acceptor, respectively, although the correlation is not perfect due to spectral overlap of the dyes and other experimental details (see Fig. 2 legend). Single-color emission can result from (*i*) denatured DNA molecules (the melting can occur during the sample preparation); (*ii*) still hybridized molecules, but with a nonactive donor or acceptor molecule (due to photobleaching or orientation with respect to

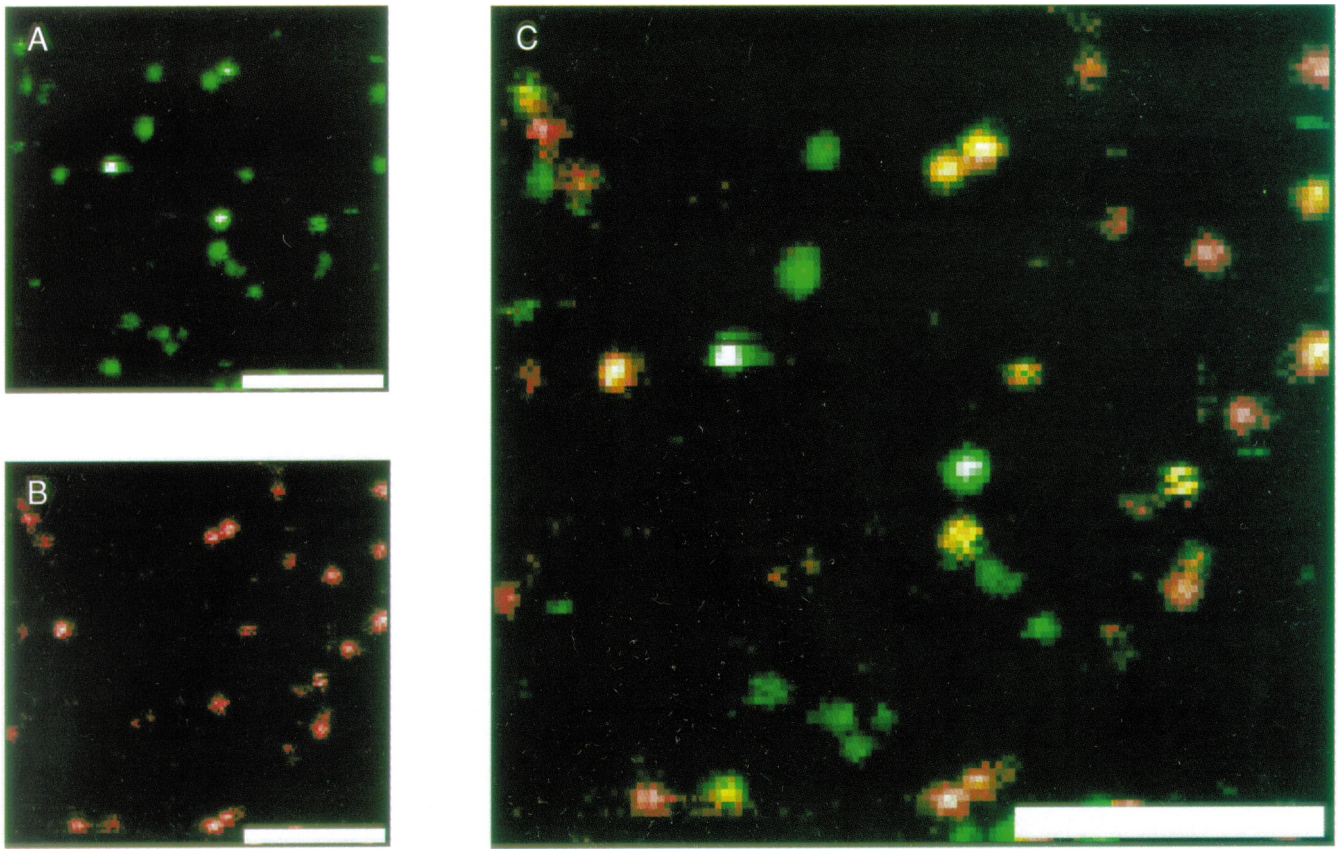

FIG. 2. Two-color near-field scanning fluorescence images of doubly labeled DNA molecules, obtained with linearly polarized excitation light (along the white 1 μm scale bar). The donor channel image (*a*) is colored in green. The acceptor channel image (*b*) is colored in red. The images are 128 × 128 pixels, 20 nm/pixel, with an integration time per pixel of 10 ms. Both images were obtained *simultaneously* by separating the emission with a dichroic mirror at 600 nm and collecting the signals on two APD detectors. The two color images are overlaid and their red-green-blue values are added together to form the composite image of *c*. There is a considerable amount of cross-talk between the channels due to dichroic polarization sensitivity and due to spectral overlap of the two fluorophores. To minimize this cross-talk, narrow bandpass filters are placed in front of the detectors. The number of red, green, and yellow spots can be used as a crude estimate of the degree of DNA hybridization on the dry surface.

the excitation polarization); and (*iii*) red features can also result from complete energy transfer. Yellow spots in Fig. 2*c* arise when donor and acceptor have comparable emission and signify that the DNA molecule still holds the two fluorophores together even on the dry surface, such that they are both under the near-field probe. Such emission from a distinct spot in space is evidence for two-color emission from a doubly labeled molecule (or possibly two single-stranded DNAs in very close proximity labeled with a single-donor and single-acceptor).

In a similar way to the data presented in Fig. 1, to acquire spectra of doubly labeled DNA, the near-field probe was positioned over a yellow spot and its emission spectrum was taken. It was found that yellow spots had broad and most often two-peaked spectrum that is quite distinct from that of a single fluorophore (donor-only or acceptor-only).

Such a typical double peak spectrum from TMR-20-TR pair is shown in Fig. 3*a* (gray circles). These data were fit (solid line) by a superposition of the individual donor-only (dashed line) and acceptor-only (dotted line) spectra. Fitting was accomplished by starting with the average donor-only and acceptor-only two-Gaussian curve-fits (see Fig. 1 *Insets*) and allowing the FWHM and the peak positions to vary within their experimentally determined limits.

The excellent fit of Fig. 3*a* using typical single molecule spectra indicates that any interaction between the TMR and the TR is sufficiently weak and that the individual emission characteristics are not perturbed. This weak coupling indicates that Förster's theory (1) should be applicable to an analysis of energy transfer between the donor and acceptor on the TMR-20-TR. We note, however, that the spectrum and excited state lifetime can be affected by the metallic coating of the NSOM tip (11, 12, 13). At room temperature, the tip has little effect on single molecule spectra, although it can have a significant effect on the lifetime. Alteration of lifetime can affect the efficiency of energy transfer, although such an effect would not be expected to invalidate the underlying Förster theory. Even though the tip effect on energy transfer was not pursued in this work, we note that quantitative measurements of distances and their relation to energy transfer efficiencies would require investigation of the tip effect.

In contrast to the TMR-20-TR data shown in Fig. 3*a*, the typical two-color emission spectra for the TMR-10-TR sample, as shown in Fig. 3*b*, cannot be fit well by a superposition of the donor and acceptor spectra. To achieve the fit shown in Fig. 3*b*, it was necessary to use the extreme values for the FWHM of the donor-only and acceptor-only base functions (see Fig. 1). This contrast between 10-mer and 20-mer samples is highly reproducible. A strong coupling, or Dexter exchange, may be present in the 10-mer case (14). No evidence for strong coupling was observed in solution.

Two-color emission such as in Fig. 3 can arise either from independent emission of the donor and the acceptor (acceptor absorption at the 514.5-nm excitation wavelength is non-zero) or due to excitation of the donor, followed by energy transfer to the acceptor. Here, we show how the dynamics of the photodestruction (photobleaching) of the fluorophores can assist us in determining the presence and extent of energy transfer. We distinguish between two cases: (*i*) either the acceptor photobleaches first or (*ii*) the donor photobleaches first. If the acceptor photobleaches first (and at the same time

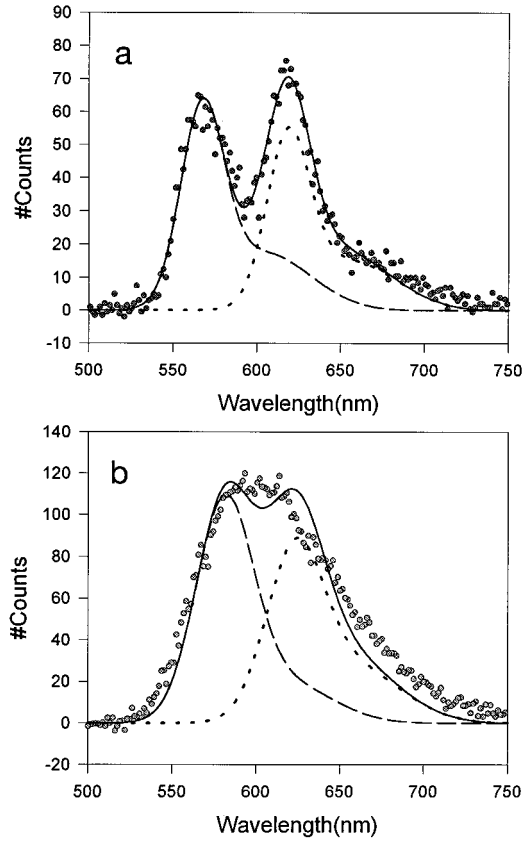

FIG. 3. Typical spectra (gray circles) obtained on single TMR-20-TR (*a*) and single TMR-10-TR (*b*) samples. A small background remains after bleaching of both molecules, and has been subtracted. TMR and TR base-functions are used to fit *a* and *b*. The data in *a* can be fit well (solid line) to a superposition of donor (dashed-line) and acceptor (dotted-line) emission, while the broad and featureless spectrum in *b* cannot be fit well (see text).

stops absorbing light), then donor emission will increase if energy transfer is present, because the de-excitation channel provided by energy transfer is eliminated. If, however, the two-color emission is simply due to independent excitation and emission of the two fluorophores, donor emission will remain at the same intensity after bleaching of acceptor. In the second case, where the donor photobleaches first, the remaining direct excitation component of the acceptor emission can be measured and subtracted from the original two-color spectra. A non-zero difference spectra at the acceptor-emission component is evidence of energy transfer.

The extent of energy transfer can also be determined. If the acceptor photobleaches first, the efficiency of energy transfer is $E = (I_D - I_{D_A})/(I_D - \alpha \cdot I_{D_A})$, where I_{D_A} is the integrated donor emission in the presence of acceptor (before acceptor photobleaching), I_D is the integrated donor emission after acceptor photobleaching, and $\alpha(<1)$ is the fraction of acceptor absorption that remains after photobleaching. Note that the α term is necessary because a photobleached acceptor (i.e., nonemitting) may potentially still absorb light. In the limit where $\alpha = 0$, this formula is equivalent to the conventional ensemble FRET formula used to measure E by a decrease in donor intensity. In the case where the donor photobleaches first, the efficiency of energy transfer is $E = [1 + (I_{D_A}/I_{A_D}) \cdot (\phi_A/\phi_D)]^{-1}$, where I_{D_A} is the integrated area of the donor emission in the presence of an unbleached acceptor, I_{A_D} is the integrated area of the sensitized emission of the acceptor, and ϕ is the quantum yield for the donor-only or acceptor-only complexes. (Sensitized emission is defined as acceptor emission due only to energy transfer—i.e., not including the fluorescence due to direct excitation.) This equation is identical to the equation used in ensemble-FRET when measuring energy transfer by sensitized emission of the acceptor.

Fig. 4 shows two cases of energy transfer between a single

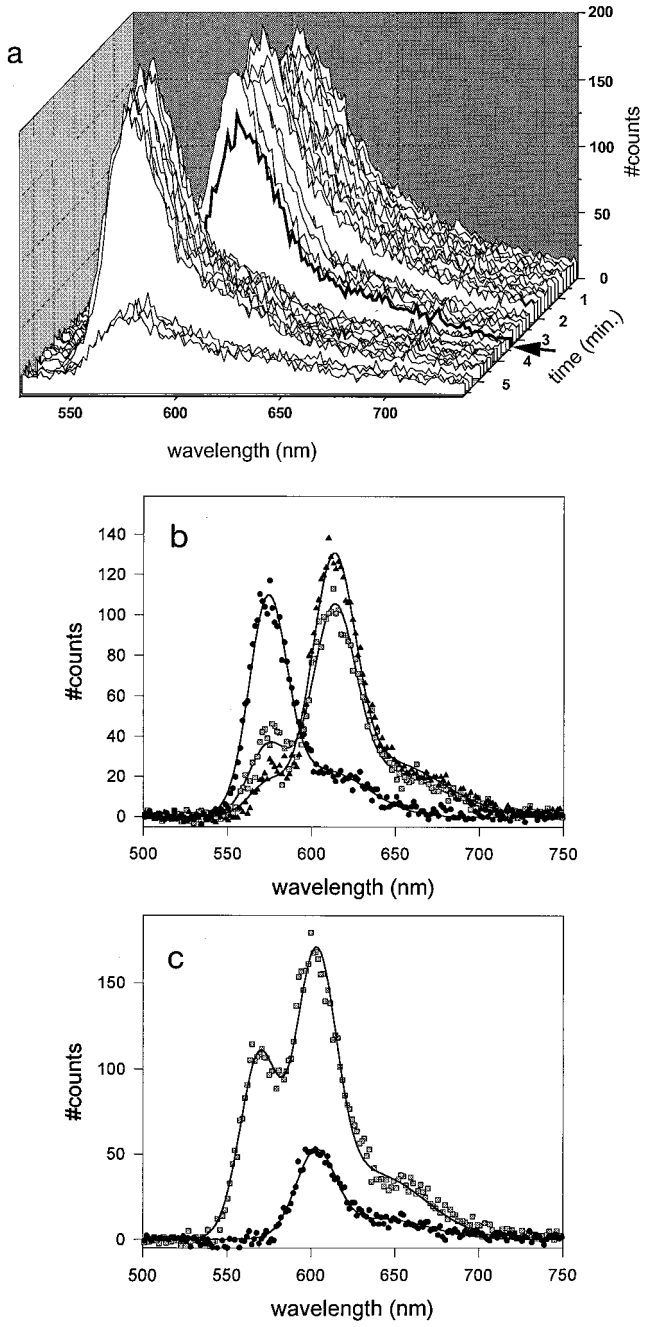

FIG. 4. (*a*) Time evolution of a single TMR-20-TR pair (see text for discussion). After the 60th scan (5 min), both donor and acceptor are bleached and a small and constant background remains. This background is due to autofluorescence from the NSOM tip and possibly fluorescence from distant molecules, which may be excited by reflected excitation light. (*b*) Background-subtracted spectra of *a* in 39th, 40th, and 41st scan (black triangles, gray squares, and black circles, respectively). Each spectrum is fit with a combination of donor and acceptor spectra and the fits are shown in solid lines. From the fit, it is determined that the acceptor photobleached at 4 s within the 40th scan, and E is at least 85%. (*c*) Background-subtracted spectra on another TMR-20-TR pair. The first spectrum (5 s/spectrum) is plotted in gray squares and the second spectrum is plotted in black circles. Here, the donor photobleached within the first scan, leaving a reduced acceptor emission which then photobleached at the 16th scan. Solid lines are fit to the spectra. E is calculated to be 53% (see text).

donor and a single acceptor. In Fig. 4 *a* and *b*, the acceptor photobleaches first; in Fig. 4*c*, the donor photobleaches first. Fig. 4*a* shows a continuous series of 5-s spectral scans of one donor-acceptor pair. Fig. 4*b* highlights those scans in Fig. 4*a* where sudden transitions occurred. Initially (black triangles in Fig. 4*b*), fluorescence is predominantly due to acceptor emission (peak at 613 nm) with a small donor component (peak at 574 nm). During the 40th scan (200 s, shown as an arrow in Fig. 4*a* and as gray squares in Fig. 4*b*), the acceptor photobleaches and the donor emission rises. The 41st scan (black circles in Fig. 4*b*) shows the final donor intensity after acceptor photobleaching. The sudden photobleaching of the acceptor emission is evidence for a single acceptor molecule, and the corresponding sudden rise in donor emission is strong evidence that the acceptor absorption is significantly reduced after photobleaching and that energy transfer was occurring before the acceptor photobleached. The sudden donor photobleaching at the 60th scan (300 s) is evidence that donor emission is arising from a single donor molecule. From the difference in donor emission intensity between scans 39 and 41 (before and after photobleaching of acceptor), we estimate the energy transfer efficiency to be 85%. The extent of energy transfer is higher if some of the acceptor absorption remains after its emission quenching ($\alpha > 0$). We have observed a simultaneous increase in donor emission with the photobleaching of the acceptor on three other different TMR-20-TR pairs. We used the same fitting procedure as discussed above and estimated energy transfer efficiencies of 16%, 30%, and 51% on these additional pairs. This wide range in efficiencies (16–85%) is due to variances in distances, κ^2, quantum yields, and spectral overlap among pairs and is a manifestation of the inhomogeneity that comes from different local environments. In particular, distance variation can come from the flexible 6-carbon linkages that can bring the dyes closer together, or farther away than their points of attachment on the DNA. The drying process on the APS-treated glass can also contribute to variation in distances. For the particular 20-mer in Fig. 4 *a* and *b* it is difficult, although not impossible, to explain the 85% energy transfer if one assumes the DNA is in its usual B-form configuration. For this to be the case, the dyes must be aligned optimally for energy transfer ($\kappa^2 = 4$), the donor quantum yield must be one (leading to an R_o of 70 Å), and the flexible linkers must bring the dyes as close as possible, all of which would lead to a dye–dye separation of 52 Å. It is therefore likely that the DNA on the surface, for this particular case, is not in its usual B-form. It may be bent by its interaction with the APS glass or may be unhybridized and a donor and acceptor molecule from separate DNA single strands are lying in close proximity to each other.

An alternative explanation for the data in Fig. 4*b*, which does not involve energy transfer, can be postulated if three conditions are met: the two fluorophores have orthogonal dipole orientations; the acceptor absorption dipole is parallel to the excitation polarization; and the DNA molecule holding the two chromophores undergoes 90° rotation around its long axis. This explanation is unlikely, however, because it requires three simultaneous and independent conditions to be met and because we have observed that sudden large decreases in molecular emission are not caused by rotation (data not shown). This was done by simultaneously analyzing single molecule emission at two cross polarizations. Rotation would lead to anti-correlated signals; however, we observed a correlated decrease in both signals, indicating that the sudden decreases were due to photobleaching.

Fig. 4*c* illustrates an example of energy transfer where the donor photobleaches first. The sudden photobleaching of the donor, followed at a later point by sudden photobleaching of the acceptor, is evidence that we are looking at a single donor and a single acceptor. After donor bleaching, a small but significant acceptor emission remains (black circles), which is due to direct excitation. By subtracting this direct excitation component from the initial spectrum (gray squares) and by comparing the remaining areas due to donor and acceptor emission, we calculate the energy transfer efficiency to be 53%, assuming the donor and acceptor quantum yields are equal.

The data in Fig. 4 show two particular cases. As mentioned before, donor emission was observed to increase upon acceptor photobleaching in four cases. We have also observed many cases where photobleaching of either donor or acceptor does not cause a change in emission of the other, indicating no energy transfer, possibly due to unfavorable dipole orientations for energy transfer. We have also found in many other cases that both colors photobleached simultaneously. In this case we cannot determine if, or to what extent, energy transfer is present. To increase the yield of usable data, the acceptor could be intentionally photobleached with a second excitation wavelength. In addition, to quantitatively determine distances with spFRET, the dipole moment orientations of the individual molecules need to be measured, since the fluorophores maintain a relatively fixed orientation on the dry surface and the assumption of $\kappa^2 = 2/3$ is not valid. The effect of the metallic coating of the tip on the energy transfer also needs to be investigated before spFRET can be used for accurate distance determination.

In conclusion, we have demonstrated that energy transfer can be measured on a single donor-acceptor pair. spFRET can potentially be extended to solution-based measurements, where it has the potential to become an important technique for dynamic measurements, particularly for monitoring conformational changes of biological macromolecules (molecular motors, and protein–protein and protein–DNA interactions). Recently, the ability to operate NSOM in aqueous solution has been reported (15). Single-molecule spectroscopic techniques with resolution from 10 to 500 nm have recently become an important tool in understanding conformational changes of molecules (16–18). spFRET, which is sensitive to shorter distances, can potentially complement these other single-molecule techniques.

We thank J. K. Trautman, X. S. Xie, and E. Betzig for helpful discussions; P. Frantz for help with the APS glass preparation; and D. Botkin and M. Salmeron for helpful advice. This work was supported by the Laboratory Directed Research and Development Program of Lawrence Berkeley National Laboratory under U.S. Department of Energy Contract DE-AC03–76SF00098 and by the Office of Naval Research under Contract N00014–95-F-0099. Th.E. was supported by the Swiss National Science Foundation and by the CIBA–Geigy Foundation. P.R.S. was supported by National Institutes of Health Grant R01 GM 41911 and by the Office of Energy Research, Office of Health and Environmental Research of the Department of Energy, under Contract DE AC03–76SF0009.

1. Förster, T. (1965) in *Modern Quantum Chemistry*, ed. Sinanoglu, O. (Academic, New York), pp. 93–137.
2. Stryer L. & Haugland, R. P. (1967) *Proc. Natl. Acad. Sci. USA* **58,** 719–730.
3. Cantor, C. R. & Schimmel, P. R. (1980) *Biophysical Chemistry* (Freeman, San Francisco), Vol. 2.
4. Selvin, P. R. (1995) *Methods Enzymol.* **246,** 300–333.
5. Clegg, R. M. (1992) *Methods Enzymol.* **211,** 353–388.
6. Pohl, D. W., Denk, W. & Lanz, M. (1984) *Appl. Phys. Lett.* **42,** 651–653.
7. Lewis, A., Isaacson, M., Harootunian, A. & Muray, A. (1984) *Ultramicroscopy* **13,** 227–230.
8. Betzig, E. & Trautman, J. K. (1992) *Science* **257,** 189–191.
9. Betzig, E. & Chichester, R. J. (1993) *Science* **262,** 1422–1424.
10. Trautman, J. K., Macklin, J. J., Brus, L. E. & Betzig, E. (1994) *Nature (London)* **369,** 40–42.
11. Xie, X. S. & Dunn, R. C. (1994) *Science* **265,** 361–363.
12. Ambrose, W. P., Goodwin, P. M., Martin, J. C. & Keller, R. A. (1994) *Science* **265,** 364–366.
13. Bian, R. X., Dunn, R. C., Xie, X. S. & Leung, P. T. (1995) *Phys. Rev. Lett.* **75,** 4772–4775.
14. Dexter, D. L. (1953) *J. Chem. Phys.* **21,** 836–850.
15. Moyer, P. J., (1995) in *Third Tropical Meeting on Near Field Optics*, Topical Meeting Digest Series (European Optical Society), Vol. 8, pp. 193–194.
16. Svoboda, K. & Block, S. M. (1994) *Annu. Rev. Biophys. Biomol. Struct.* **23,** 247–285.
17. Funatsu, T., Harada, Y., Tokunaga, M., Saito, K. & Yanagida, T. (1995) *Nature (London)* **374,** 555–559.
18. Sase, I., Miyata, H., Corrie, J. E., Craik, J. S., & Kinosita, K., Jr. (1995) *Biophys. J.* **69,** 323–328.